

# Cancers adapt to their mutational load by buffering protein misfolding stress

Susanne Tilk<sup>1\*</sup>, Judith Frydman<sup>1</sup>, Christina Curtis<sup>2,3,4\*</sup>, Dmitri Petrov<sup>1,4\*</sup>

<sup>1</sup>Department of Biology, Stanford University, Stanford, CA, USA.

<sup>2</sup>Department of Medicine, Division of Oncology, Stanford University School of Medicine, Stanford, CA, USA

<sup>3</sup>Department of Genetics, Stanford University School of Medicine, Stanford, CA, USA.

<sup>4</sup>Stanford Cancer Institute, Stanford University School of Medicine, Stanford, CA, USA.

\*Correspondence to:

[tilk@stanford.edu](mailto:tilk@stanford.edu), [cncurtis@stanford.edu](mailto:cncurtis@stanford.edu), [petrov@stanford.edu](mailto:petrov@stanford.edu)

## Abstract

In asexual populations that don't undergo recombination, such as cancer, deleterious mutations are expected to accrue readily due to genome-wide linkage between mutations. Despite this mutational load of often thousands of deleterious mutations, many tumors thrive. How tumors survive the damaging consequences of this mutational load is not well understood. Here, we investigate the functional consequences of mutational load in 10,295 human tumors by quantifying their phenotypic response through changes in gene expression. Using a generalized linear mixed model (GLMM), we find that high mutational load tumors up-regulate proteostasis machinery related to the mitigation and prevention of protein misfolding. We replicate these expression responses in cancer cell lines and show that the viability in high mutational load cancer cells is strongly dependent on complexes that degrade and refold proteins. This indicates that upregulation of proteostasis machinery is causally important for high mutational burden tumors and uncovers new therapeutic vulnerabilities.

## 37 Introduction

38 Cancer develops from an accumulation of somatic mutations over time. While a  
39 small subset of these mutations drive tumor progression, the vast majority of remaining  
40 mutations, known as passengers, don't help and might hinder cancer growth. The role  
41 that passengers play in tumor progression has traditionally received little attention  
42 despite their abundance and variation across cancer types. The number of passengers  
43 in a tumor can vary by over four orders of magnitude, even within the same cancer type,  
44 from just a few to tens of thousands of point mutations<sup>1</sup>.

45 Whether these passengers are neutral or damaging to tumors has long been a  
46 matter of debate<sup>2-10</sup>. Some have argued that passengers are functionally unimportant to  
47 tumors given that most non-synonymous mutations are not removed by negative  
48 selection in somatic tissues<sup>2,3</sup>. This is in direct contrast to the human germ-line, where  
49 non-synonymous mutations are functionally damaging to most genes<sup>11</sup> and signals of  
50 negative selection are pervasive<sup>3</sup>. The common explanation for why damaging protein-  
51 coding mutations are removed in the human-germline but maintained in somatic tissues  
52 is that most genes are only important for multi-cellular function at the organismal level  
53 (e.g. during development), but not during somatic growth<sup>2,12</sup>.

54 However, the notion that non-synonymous mutations are only selectively neutral  
55 in somatic tissues is surprising given their known functional consequences in the germ-  
56 line. Non-synonymous mutations are known to be damaging in the human germ-line  
57 due to their effects on protein folding and stability<sup>13</sup>, which ought to be shared between  
58 somatic and germline evolution. An alternative explanation is that non-synonymous  
59 mutations are indeed damaging in somatic evolution, but negative selection is too  
60 inefficient at removing them due to linkage effects driven by the lack of recombination in  
61 somatic cells<sup>10</sup>. Without recombination to break apart combinations of mutations,  
62 selection must act on beneficial drivers and deleterious passengers that arise in the  
63 same genome together. This makes it less efficient for selection to individually favor  
64 beneficial drivers or remove deleterious passengers<sup>14</sup>. As a result, a substantial number  
65 of weakly damaging passengers can accrue in cancer due to inefficient negative  
66 selection over time. In support of this model, tumors with very small numbers of  
67 passengers – where linkage effects are expected to be negligible – have recently been  
68 shown to exhibit signatures of negative selection and weed out damaging non-  
69 synonymous mutations<sup>10</sup>. In contrast, the remaining majority (>95%) of tumors, which  
70 contain much larger numbers of linked mutations, display patterns of inefficient negative  
71 selection. This provides evidence in favor of the inefficient selection model and implies  
72 that most tumors carry a correspondingly large deleterious mutational load.

73 If individual passengers are in fact substantially damaging in cancer, successful  
74 tumors with thousands of linked mutations must find ways to maintain their viability by  
75 mitigating this large mutational load. While paths to mitigation are difficult to predict for  
76 non-coding mutations, tumors with mutations in protein-coding genes are expected to  
77 minimize the damaging phenotypic effects of protein mis-folding stress. Here, we  
78 investigate this hypothesis by analyzing tumor tissues with paired mutational and gene  
79 expression profiles to assess how the physiological state of cancer cells change as they  
80 accumulate protein coding mutations. Using a general linear mixed effects regression  
81 model (GLMM), we leverage variation across 10,295 tumors from 33 cancer types and  
82 find that complexes that re-fold proteins (chaperones), degrade proteins (proteasome)

83 and splice mRNA (spliceosome) are up-regulated in high mutation load tumors. We  
84 validate these results by showing that similar physiological responses occur in high  
85 mutational load cancer cell lines as well. Finally, we establish a causal connection by  
86 showing that high mutational load cell lines are particularly sensitive when proteasome  
87 and chaperone function is disrupted through downregulation of expression via short-  
88 hairpin RNA (shRNA) knock-down or targeted therapies. Collectively, these data  
89 indicate that the viability of high mutational load tumors is strongly dependent on the up-  
90 regulation of complexes that degrade and refold proteins, revealing a generic  
91 vulnerability of cancer that can potentially be therapeutically exploited.

## 92 Results

### 93 **Quantifying transcriptional response to mutational load in human tumors.**

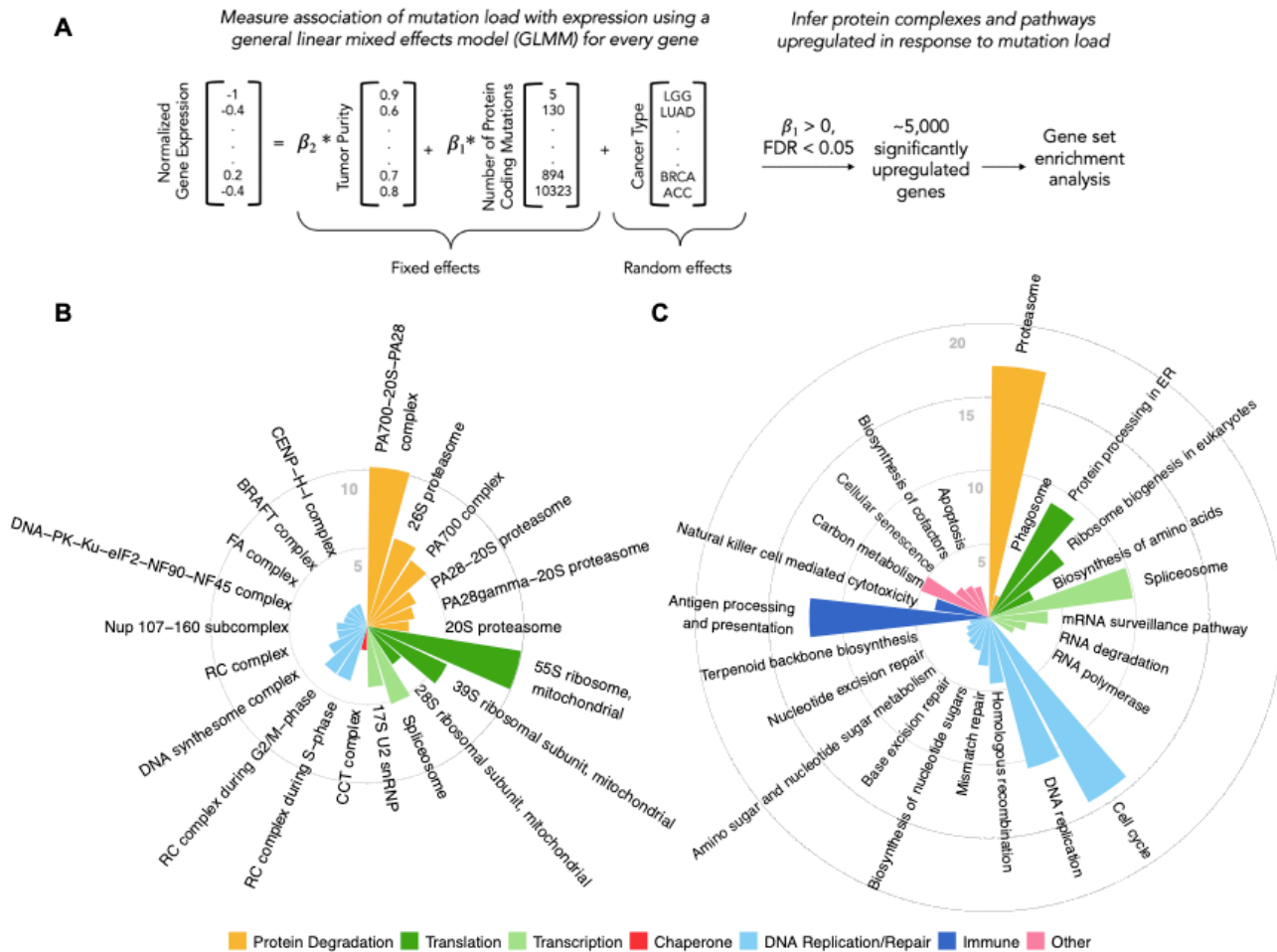
94  
95 We first performed a genome-wide screen to systematically identify which genes  
96 are transcriptionally upregulated in response to mutational load in human tumors. To do  
97 so, we utilized publicly available whole-exome and gene expression data from 10,295  
98 human tumors across 33 cancer types from The Cancer Genome Atlas (TCGA)<sup>15,16</sup>. We  
99 considered multiple classes of mutations to define mutational load and investigated their  
100 degree of collinearity, focusing on protein-coding regions since the use of whole-exome  
101 data limits the ability to accurately assess mutations in non-coding regions. We find that  
102 there is a high degree of collinearity among synonymous, non-synonymous and  
103 nonsense point mutations in protein coding genes ( $R > 0.9$ ) but weak collinearity  
104 between point mutations and copy number alterations ( $R < 0.05$ ) (Supplemental Figure  
105 1). Thus, we decided to focus on the aggregate effects of protein-coding mutations and  
106 for all analyses defined mutational load as  $\log_{10}$  of the total number of point mutations in  
107 protein-coding genes. For simplicity, we used all mutations rather than focusing only on  
108 passenger mutations since identifying genuine drivers against a background of linked  
109 passenger events can be difficult, especially for tumors with many mutations.

110 Since gene expression can vary across tumors due to many factors, such as  
111 cancer type, tumor purity and other unknown factors, we utilized a generalized linear  
112 mixed model (GLMM) to measure the association of mutational load and gene  
113 expression while accounting for these potential confounders (Fig. 1A). Within the  
114 GLMM, tumor purity and mutational load were modeled as fixed effects whereas cancer  
115 type was modeled as a random effect since it varies across groups of patients and can  
116 be interpreted as repeated measurements across groups. The following GLMM was  
117 applied separately to each gene,

$$118 \quad Y \sim \beta_0 + \beta_1 X_1 + \beta_2 X_2 + v + e$$

119  
120 where  $Y$  is a vector of normalized expression values across all tumors,  $\beta_0$  is the fixed  
121 intercept,  $\beta_1$  is the fixed slope for the predictor variable  $X_1$  which is a vector of mutational  
122 load values for each tumor,  $\beta_2$  is the fixed slope for the predictor variable  $X_2$  which is a  
123 vector of the purity of each tumor,  $v$  is the random intercept for each cancer type, and  $e$   
124 is a Gaussian error term (Methods).

125 Using this approach, we applied the GLMM to all tumors in TCGA and identified  
 126 5,330 genes that are significantly up-regulated in response to mutational load ( $\beta_1 > 0$ ,  
 127 FDR < 0.05). Next, we linked these genes to cellular function by performing gene set  
 128 enrichment to known protein complexes (CORUM database<sup>17</sup>, Fig. 1B) and pathways  
 129 (KEGG database<sup>18</sup>, Fig. 1C) using gprofiler2<sup>19</sup>. As expected for tumors with many  
 130 mutations, pathways and protein complexes related to cell cycle, DNA replication and  
 131 DNA repair were enriched in tumors with a high mutational load. However, some of the  
 132 most significant enrichment terms were for protein complexes and pathways that  
 133 regulate translation (mitochondrial ribosomes), protein degradation (proteasome  
 134 complex), and protein folding (CCT complex/HSP60), consistent with the hypothesis  
 135 that high mutational load tumors experience protein misfolding stress. Surprisingly, we  
 136 also found that the spliceosome, a large protein complex that regulates alternative  
 137 splicing in cells, is up-regulated in response to mutational load. This suggests that  
 138 transcription itself could also be regulated in response to protein misfolding stress, as  
 139 seen in other studies<sup>20,21</sup>.



140  
 141 **Figure 1. General linear mixed effects model (GLMM) identifies protein complexes and pathways**  
 142 **up-regulated in response to mutational load in human tumors. (A)** Overview of the GLMM used to  
 143 measure the association of mutation load with gene expression while controlling for potential co-variables  
 144 (purity and cancer type). Genes with a significant, positive  $\beta_1$  regression coefficient and false discovery

145 rate (FDR) < 0.05 are used for gene set enrichment analysis. **(B-C)** Circular bar plots of protein  
146 complexes from the CORUM database (left) and pathways from the KEGG database (right) that are  
147 significantly enriched ( $p < 0.05$ ) in response to mutational load. Length of bars denote negative log<sub>10</sub> of  
148 adjusted  $p$ -value and colors denote broad functional groups enriched in both databases.

149

150

## 151 **Gene silencing through alternative splicing in high mutational load tumors.**

152

153 We next investigated in detail how these protein complexes could mitigate the  
154 damaging effects of protein misfolding in high mutational load tumors by examining the  
155 role of the spliceosome in gene silencing. We hypothesized that the up-regulation of the  
156 spliceosome in high mutational load tumors prevents further protein misfolding by  
157 regulating pre-mRNA transcripts to be degraded rather than translated. The down-  
158 regulation of gene expression via alternative splicing events, such as intron retention, is  
159 one known mechanism to silence genes by funneling transcripts to mRNA decay  
160 pathways.<sup>22–24</sup>

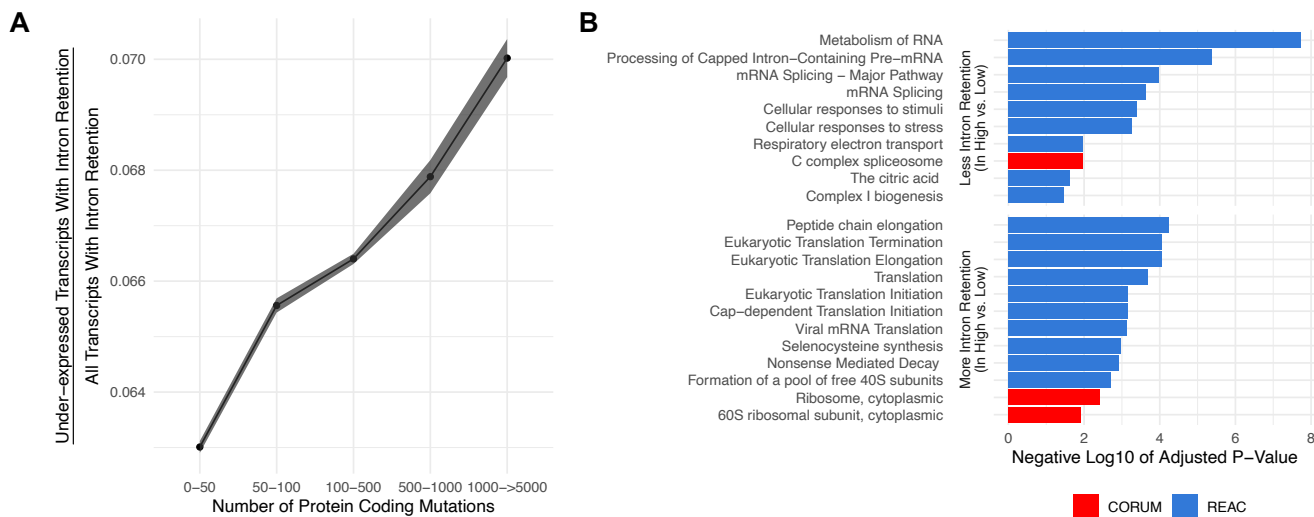
161 To test whether gene expression is down-regulated in high mutational load  
162 tumors through intron retention, we utilized previously called alternative splicing events  
163 in TCGA<sup>25</sup>. Alternative splicing events within this dataset were quantified through a  
164 metric called *percent spliced in* or PSI. PSI is calculated as the number of reads that  
165 overlap the alternative splicing event (e.g. for intron retention, either at intronic regions  
166 or those at the boundary of exon to intron junctions) divided by the total number of  
167 reads that support and don't support the alternative splicing event. Thus, PSI estimates  
168 the probability of alternative splicing events only at specific exonic boundaries in the  
169 entire transcript population without requiring information on the complete underlying  
170 composition of each full length-transcript.

171 Using these alternative splicing calls, we reasoned that if a transcript contains an  
172 intron retention event and is downregulated in expression, the transcript is more likely to  
173 have been degraded by mRNA decay pathways. For all genes, we first quantified  
174 whether intron retention events were present based on a threshold value >80% PSI. For  
175 each gene with an intron retention event, we quantified whether the expression of the  
176 same gene was under-expressed. Each gene was counted as under-expressed if it was  
177 one standard deviation below the mean expression within the same cancer type. To  
178 control for mutations that might affect patterns of expression, (i.e., expression  
179 quantitative trait loci or eQTL effects), alternative splicing events that contained a point  
180 mutation within the same gene were removed from the analysis (which only represent  
181 ~1% of intron retention events across all tumors; Methods). We find that relative to all  
182 transcripts with intron retention events, the number of transcripts that are under-  
183 expressed increases with tumor mutational load (Fig. 2A), suggesting that the degree of  
184 intron-retention driven mRNA decay is elevated in high mutational load tumors. This  
185 trend is robust to other PSI value thresholds (>50-90% PSI), even for other alternative  
186 splicing events (e.g., exon skipping, mutually exclusive exons, etc.) and when not  
187 filtering for potential eQTL effects (Supplemental Figure 2 and 3).

188 We next investigated which genes are more likely to be silenced through mRNA  
189 decay between low and high mutational load tumors. For each intron retention event,  
190 we calculated whether PSI values were significantly different in low mutational load  
191 tumors (<10 total protein-coding mutations) compared to high mutational load tumors



192 (>1000 total protein-coding mutations) using a t-test. This approach identified 606 and  
 193 201 genes that have more and less intron retention events in high mutational load  
 194 tumors, respectively. Using gene set enrichment analysis, we find that cytoplasmic  
 195 ribosomes contain more intron retention events in high mutational load tumors,  
 196 potentially leading to their down-regulation through mRNA decay to prevent further  
 197 protein mis-folding (Fig. 2B). Genes that contain fewer intron retention events in high  
 198 mutational load tumors, which are less likely to undergo mRNA decay, are primarily  
 199 related to mRNA splicing.  
 200



201  
 202 **Figure 2. Gene silencing is elevated in high mutational load tumors likely through the coupling of**  
 203 **intron retention with mRNA decay. (A)** Counts of the number of under-expressed transcripts with intron  
 204 retention events, relative to counts of all intron retention events in tumors binned by the total number of  
 205 protein-coding mutations. Intron retention events with PSI > 80% are counted. Error bars are 95%  
 206 confidence intervals determined by bootstrap sampling. **(B)** Barplot of significant protein complexes in the  
 207 CORUM database (in red) and Reactome pathway database (in blue) with more (bottom) and less (top)  
 208 intron retention events in high mutational load tumors compared to low mutational load tumors.  
 209

## 210 Regulation of translation, protein folding and protein degradation in high 211 mutational load tumors. 212

213 Next, we investigated in detail how the remaining proteostasis complexes that  
 214 were significant in our genome-wide screen, which regulate protein synthesis,  
 215 degradation and folding, could mitigate protein misfolding in high mutational load  
 216 tumors. To do so, we expanded our gene sets to include other chaperone families, all  
 217 ribosomal complexes and proteasomal subunits (Fig. 3A). Using the GLMM framework  
 218 detailed above, we find that the expression of nearly all individual genes in chaperone  
 219 families that participate in protein folding (HSP60, HSP70 and HSP90), protein  
 220 disaggregation (HSP100), and have organelle-specific roles (ER and mitochondrial) are  
 221 significantly up-regulated in response to mutational load. Interestingly, however, small  
 222 heat shock proteins, which don't participate in protein folding or disaggregation, are  
 223 significantly down-regulated in response to increased protein coding mutations. The role

224 of small heat shock proteins is primarily to hold unfolded proteins in a reversible state  
225 for re-folding or degradation by other chaperones<sup>26</sup> and thus, could possibly be down-  
226 regulated due to their inefficiency in mitigating protein misfolding.

227 We further examined differences in expression of different structural components  
228 of the proteasome, a large protein complex responsible for degradation of intracellular  
229 proteins. Consistent with the over-expression of chaperone families that mitigate protein  
230 mis-folding, both the 19s regulatory particle (which recognizes and imports proteins for  
231 degradation) and the 20s core (which cleaves peptides) of the proteasome are up-  
232 regulated in response to mutational load in TCGA (Fig. 3A). In addition, we find that  
233 specifically mitochondrial — but not cytoplasmic — ribosome complexes are up-  
234 regulated in high mutational load tumors. As previously reported in yeast<sup>27</sup> and human  
235 cells<sup>28</sup>, mitochondrial ribosome biogenesis has been shown to occur under conditions of  
236 chronic protein misfolding as a mechanism of compartmentalization and degradation of  
237 proteins. In contrast, translation of proteins through cytosolic ribosome biogenesis has  
238 been previously characterized to be attenuated and slowed to prevent further protein  
239 mis-folding<sup>29</sup>. This decrease in expression of cytoplasmic ribosomes is also consistent  
240 with observed patterns of alternative splicing coupled to mRNA decay pathways in high  
241 mutational load tumors (Fig. 2B).

242 Finally, we performed a jackknife re-sampling procedure to confirm that specific  
243 cancer types aren't driving patterns of association within the GLMM. This was achieved  
244 by removing each cancer type from the regression model one at a time, and re-  
245 calculating regression coefficients on the remaining set of samples. Overall, regression  
246 coefficients were stable across cancer types and trends were unchanged (Supplemental  
247 Figure 4). In addition, we also confirmed that patient age was not driving patterns of  
248 association of mutational load and gene expression within the GLMM (Supplemental  
249 Figure 5). Taken together, this suggests that protein re-folding, protein disaggregation,  
250 protein degradation, and down-regulation of cytoplasmic translation are potential  
251 mechanisms to mitigate and prevent protein misfolding in high mutational load tumors.

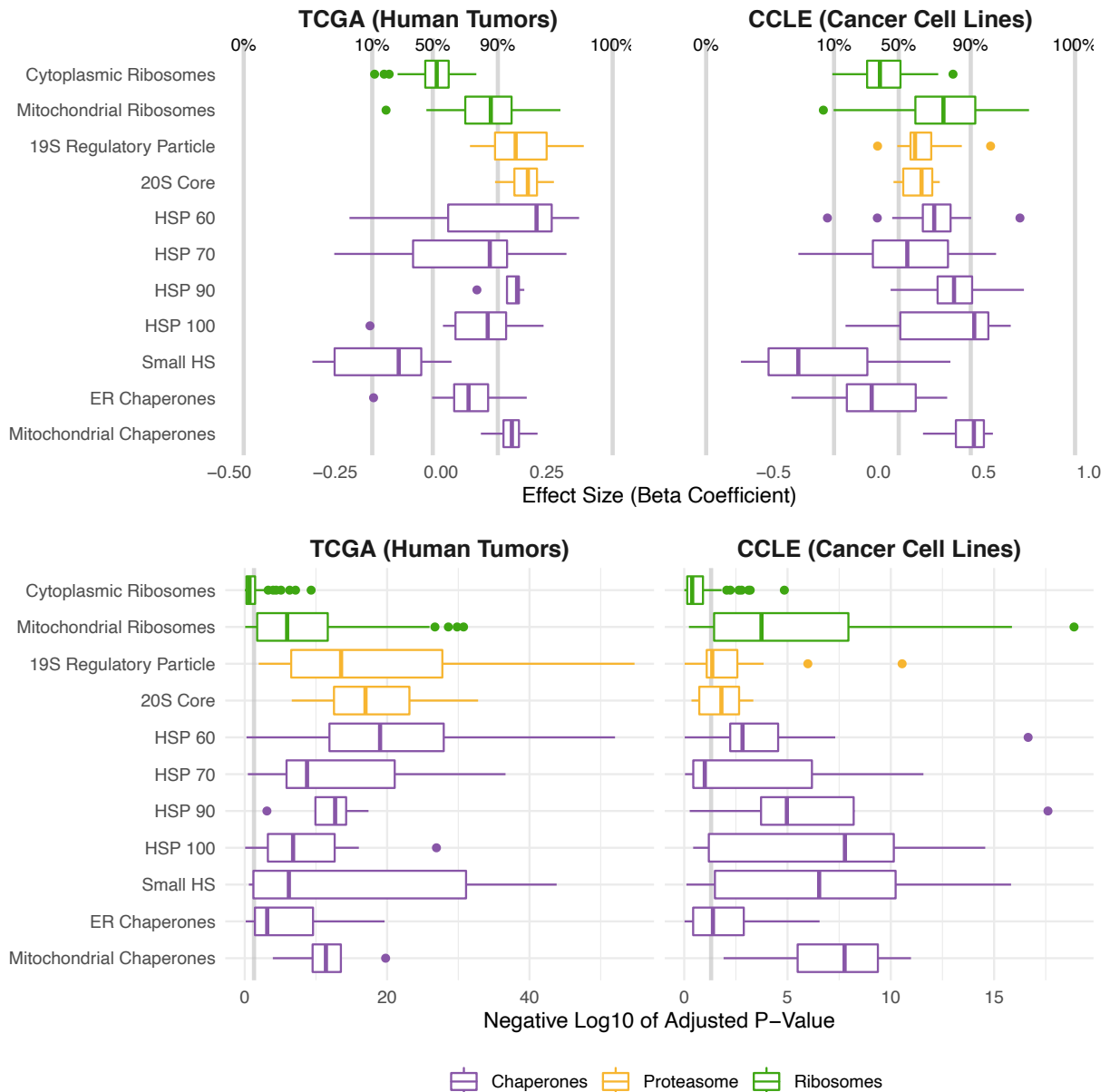
252

### 253 **Validating proteostasis expression responses in cancer cell lines and** 254 **establishing a causal connection through perturbation experiments.**

255

256 We next sought to validate these results by examining whether the expression  
257 patterns observed in human tumors replicate within cancer cell lines from the Cancer  
258 Cell Line Encyclopedia (CCLE)<sup>30</sup>. Unlike TCGA, samples within each cancer type in  
259 CCLE can be small and are unbalanced (i.e., some cancer types have <10 samples and  
260 others have >100 samples). Since GLMMs may not be able to estimate among-  
261 population variance accurately in these cases<sup>31</sup>, we utilized a simple generalized linear  
262 model (GLM) instead to measure the effect of mutational load on patterns of expression  
263 without over-constraining the model. Indeed, we find that expression patterns seen in  
264 human tumors broadly replicate in cancer cell lines (Fig. 3). Similar to the expression  
265 analysis in TCGA, we also confirmed through a jackknife re-sampling procedure that  
266 specific cancer types aren't driving patterns of association within the GLM  
267 (Supplemental Figure 6). Overall, this indicated that the expression patterns observed  
268 are cell autonomous (i.e., independent of organismal effects such as the immune  
269 system, age or microenvironment) and consistent across high mutational load cancer

270 cells. Importantly, it also demonstrates that cancer cell lines are a reasonable model to  
 271 causally interrogate these effects further through functional and pharmacological  
 272 perturbation experiments.  
 273



274  
 275  
 276  
 277 **Figure 3. Protein folding, degradation, and synthesis are regulated in both high mutational load**  
 278 **tumors (TCGA) and cell lines (CCLE).** Box plots of  $\beta_1$  regression coefficients (top panels) and negative  
 279  $\log_{10}$  adjusted  $p$ -values (bottom panels) measuring the association of mutation load and the expression of  
 280 individual genes in chaperone (purple), proteasome (yellow), and ribosome (green) complexes. Shown  
 281 are regression coefficients from human tumors (TCGA) on the left and cell lines (CCLE) on the right.  
 282 Percentages and grey lines on top panels show the quantile distribution of regression coefficients  
 283 measuring the association of mutational load and expression for all genes in the genome within each  
 284 dataset. Vertical grey line on bottom panels shows threshold of significance ( $p = 0.05$ ).

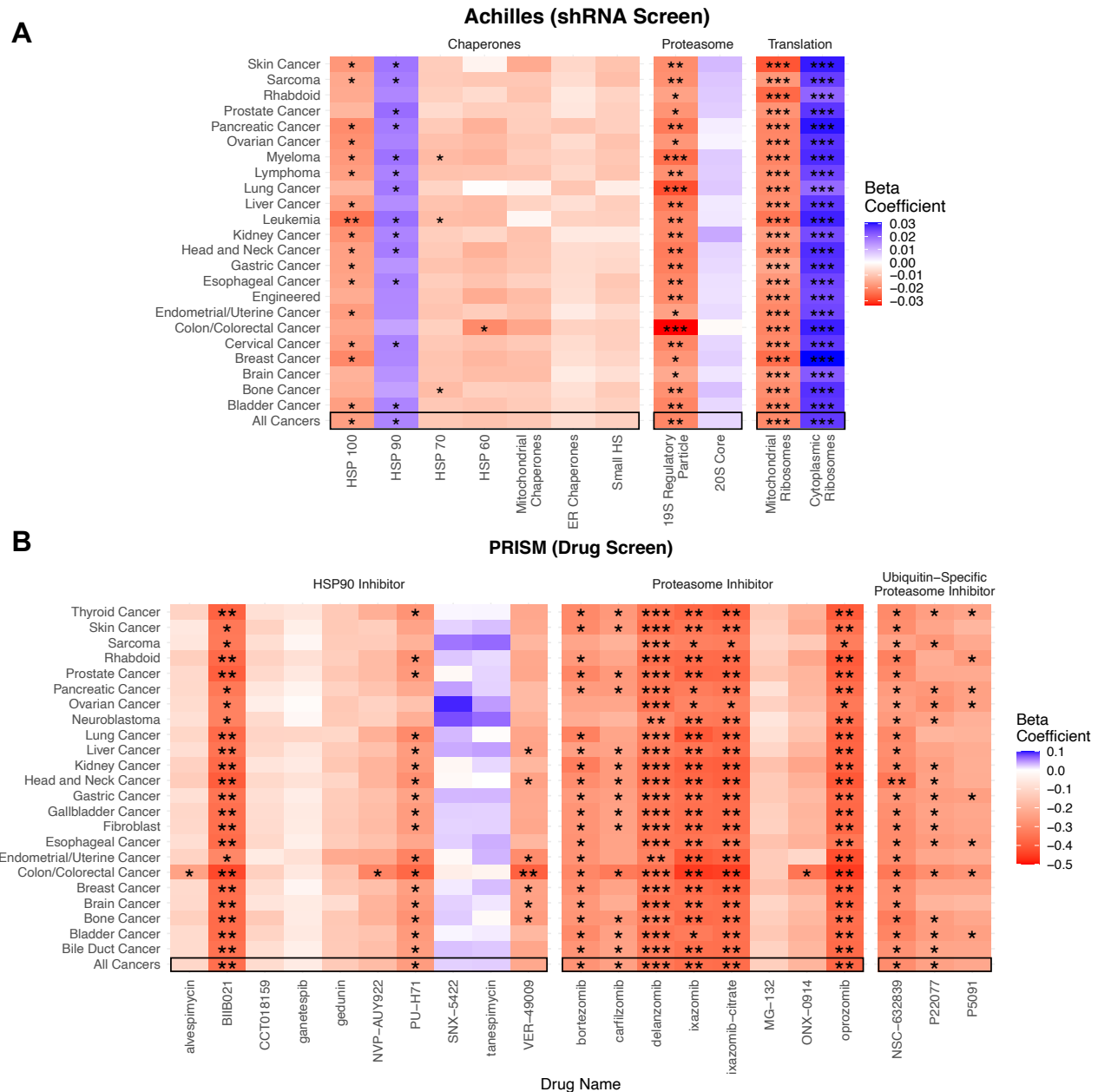


285 To establish a causal relationship between the over-expression of proteostasis  
286 machinery and maintenance of cell viability under high mutational load, we utilized  
287 expression knock-down (shRNA) estimates from project Achilles<sup>32</sup> for the same cancer  
288 cell lines as in CCLE. We sought to measure how mutational load impacts cell viability  
289 when protein complexes and gene families undergo a loss of function through  
290 expression knock-down. Since the shRNA screen was performed on an individual gene  
291 basis, we utilized a GLM framework that aggregates expression knock-down estimates  
292 of all genes within a given proteostasis gene family to jointly measure how mutational  
293 load impacts cell viability after loss of function. Specifically, we included an additional  
294 categorical variable of the gene name within each gene family to allow for a change in  
295 the intercept within each gene in the GLM when measuring the association of  
296 mutational load and cell viability after expression knock-down. In addition, we similarly  
297 evaluated whether specific cancer types were driving patterns of association within the  
298 GLM through jackknife re-sampling by cancer type (Fig. 4A).

299 Overall, we find that elevated mutational load is associated with decreased cell  
300 viability when the function of most chaperone gene families are disrupted through  
301 expression knock-down (Fig. 4A). However, only chaperones within the HSP100 family,  
302 which have the unique ability to rescue and reactivate existing protein aggregates in  
303 cooperation with other chaperone families<sup>33</sup>, show a significant negative relationship  
304 between mutational load and cell viability across almost all cancer types. Similarly, we  
305 find specificity in the vulnerability that mutational load generates when the function of  
306 the proteasome and different ribosomal complexes are disrupted (Fig. 4A). Mutational  
307 load significantly decreases cell viability only when expression knock-down of the 19s  
308 regulatory particle of the proteasome is disrupted, suggesting that targeting the protein  
309 import machinery of the proteasome is more effective than targeting the protein cleaving  
310 machinery in the 20s core. Finally, mutational load significantly increases cell viability  
311 when cytoplasmic ribosomes – which are already down-regulated in response to  
312 mutational load (Fig. 2B) – undergo a loss of function through expression knock-down.  
313 Conversely, expression knock-down of mitochondrial ribosomes significantly decreases  
314 viability with increased mutational load in cell lines, which is also consistent with the  
315 patterns of expression observed.

316 Since functional redundancy in the human genome can make expression knock-  
317 down estimates within individual genes noisy, we also examined how drugs targeting  
318 the function of whole complexes impacts viability with mutational load across all cancer  
319 types and when removing individual cancer types through jackknife re-sampling. To do  
320 so, we utilized drug sensitivity screening data in project PRISM<sup>34</sup> within CCLE and used  
321 a simple GLM to measure the association of mutational load and cell viability after drug  
322 inhibition. We find that treatment with the majority of proteasome inhibitors (6/8) and  
323 ubiquitin-specific proteasome inhibitors (2/3), which target protein degradation  
324 complexes, are significantly associated with a decrease in cell viability in high  
325 mutational load cell lines. Similarly, most HSP90 inhibitors decrease cell viability with  
326 mutational load (8/10), although only a few drugs show a significant relationship. This  
327 variability in the efficacy of drugs with similar mechanisms of action likely reflects that  
328 the efficacy to disrupt the function of proteostasis machinery is dependent on the  
329 specific molecular affinity of a compound to its target and downstream effectors. While  
330 these are the only relevant proteostasis drugs in the PRISM dataset that are currently

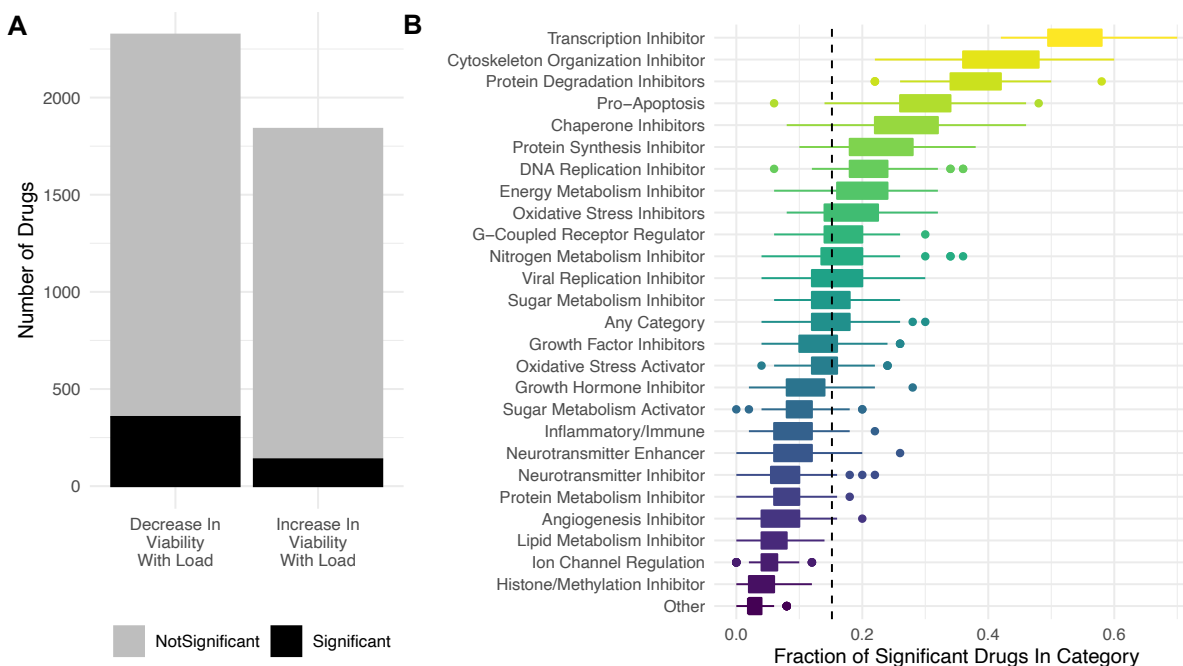
331 available, we anticipate that drugs targeting other chaperone machinery or splicing  
 332 complexes could also target other potential vulnerabilities in high mutational load  
 333 cancers. Collectively, these results indicate that elevated expression of protein  
 334 degradation and folding machinery is causally related to the maintenance of viability in  
 335 in high mutational load cell lines, and likely in high mutational load tumors by extension.



336 **Figure 4. Viability in high mutational load cell lines decreases when proteostasis machinery is**  
 337 **disrupted. (A)** Heatmap of  $\beta_1$  regression coefficients jointly measuring the association of mutational load  
 338 and cell viability after expression knockdown of individual genes in proteostasis complexes. **(B)** Heatmap  
 339 of  $\beta_1$  regression coefficients measuring the association mutational load and cell viability after inhibition of  
 340 proteostasis machinery via drugs. Both panels show how stable regression estimates are when including  
 341 all cancer types ('All Cancers') shown in black boxes and when removing each individual cancer type on  
 342 the y-axis. Colors denote a positive (blue), zero (grey), or negative (red) relationship of mutational load  
 343

344 and cell viability after expression knock-down or drug inhibition. Stars denote whether the relationship is  
 345 significant (\* =  $p < 0.05$ ; \*\* =  $p < 0.005$ ; \*\*\* =  $p < 0.0005$ ).

346  
 347 Lastly, we find that most drugs in the PRISM database do not significantly  
 348 decrease cell viability with mutational load (Fig. 5A), suggesting that high mutational  
 349 load cancer cells are not generically vulnerable to all classes of drugs. Specifically, we  
 350 find that drugs which inhibit transcription, cytoskeleton organization, protein  
 351 degradation, chaperones, protein synthesis and promote apoptosis are most effective at  
 352 targeting high mutational load cancer cells – delineating additional potential therapeutic  
 353 vulnerabilities in high mutational burden tumors (Fig. 5B).  
 354



355 **Figure 5. Targeting proteostasis machinery is a key vulnerability in high mutational load cell lines.**  
 356 **(A)** Bar plot of the number of drugs in the PRISM database significantly (black) and not significantly (grey)  
 357 associated with mutational load and cell viability using a simple generalized linear model (GLM). **(B)**  
 358 Fraction of drugs in broad functional categories significantly negatively associated with mutational load  
 359 and cell viability from the GLM. Confidence intervals were determined by randomly sampling 50 drugs in  
 360 each functional category 100 times. Dashed line is the median of randomly sampled drugs across all  
 361 categories.  
 362

363

364

365

366

## 367 Discussion

368 Here, we test the hypothesis that cancer cells regulate their proteostasis  
369 machinery to mitigate the damaging effects of passenger mutations, which can  
370 destabilize and misfold proteins. Misfolded proteins can arise from non-synonymous or  
371 nonsense passengers which cause abnormal amino acid modifications or pre-mature  
372 truncations in proteins. Even synonymous passengers, which are traditionally thought to  
373 be functionally silent, can lead to misfolding of proteins through changes in mRNA  
374 stability<sup>35</sup>, translational pausing<sup>36,37</sup>, and non-optimal codon usage.<sup>38,39</sup> As a result,  
375 protein misfolding can be damaging in cells not only due to a loss of function of the  
376 original protein, but also due to a gain in toxicity caused by the aggregation of aberrant  
377 peptides. It is intriguing to consider the possibility that the need to manage protein  
378 misfolding stress is a hallmark of somatic evolution in cancer.

379 To maintain viability by minimizing these cytotoxic effects, we find that high  
380 mutational load tumors – similar to yeast<sup>40</sup>, bacteria<sup>41,42</sup>, and viruses<sup>43</sup> – up-regulate the  
381 expression of chaperones, which allow mutated proteins that would otherwise be  
382 misfolded to retain function. We find evidence suggesting that specific chaperone  
383 families that actively participate in protein re-folding (HSP60, HSP90 and HSP70) or  
384 disaggregation (HSP100) are up-regulated in response to mutational load, while other  
385 chaperone machinery that salvage proteins (Small HS) are downregulated. In addition,  
386 we find degradation of mutated proteins through up-regulation of the proteasome to be  
387 another possible strategy high mutational load tumors use to mitigate protein misfolding  
388 stress.

389 Finally, we find additional mechanisms that high mutational load tumors use to  
390 not just mitigate but also prevent protein misfolding. By utilizing post-transcriptional  
391 processes that couple alternative splicing with mRNA decay pathways known to occur  
392 in normal human tissues<sup>22,44,45</sup>, high mutational load tumors appear to selectively  
393 prevent protein production by regulating certain pre-mRNA transcripts to be degraded  
394 rather than translated. We find evidence suggesting that the targets of this coordinated  
395 un-productive splicing are primarily related to cytoplasmic ribosomal gene expression  
396 that controls the translation of proteins, consistent with observations in other  
397 organisms<sup>46–48</sup>. Intriguingly, we find that while cytoplasmic ribosome expression is  
398 attenuated, mitochondrial ribosome biogenesis in human tumors is up-regulated in  
399 response to mutational load. This could both be another mechanism that high  
400 mutational load tumors use to compartmentalize and degrade proteins<sup>27</sup> and reflect the  
401 increased energetic demands of proteostasis maintenance<sup>49</sup>.

402 The expression responses observed here are not only consistent with protein  
403 misfolding stress in other organisms, but also cross-validate in cancer cell lines, where  
404 we find similar expression responses to mutational load. This provides further evidence  
405 of a generic, cell intrinsic phenomenon occurring that cannot be explained by extrinsic  
406 organismal effects, such as aging, changes in the immune system or microenvironment.  
407 Furthermore, we move beyond correlations of gene expression responses to mutational  
408 load and establish a causal connection by demonstrating that mitigation of protein  
409 misfolding through protein degradation and re-folding is necessary for high mutational  
410 load cancer cells to maintain viability through perturbation experiments via knockdown  
411 experiments with shRNA and drug profiling.

412 The results presented here have many implications. First, they suggest that while  
413 there is direct selection during somatic evolution for pathogenic drivers that allow cancer  
414 cells to continually proliferate, damaging passengers that destabilize proteins must also  
415 cause cancer cells to experience second-order indirect selection for alterations that  
416 allow tumors to overcome this proteostasis imbalance. This could occur through  
417 phenotypic plasticity, shifts in methylation and chromatin structure, or through  
418 compensatory point mutations and duplications, consistent with other studies<sup>50,51</sup>.  
419 Indeed, gene duplication, where one copy can still perform the required function while  
420 the other copy is non-functional, is another known mechanism that allows cells to  
421 maintain robustness to damaging mutations in many eukaryotic organisms<sup>52,53</sup>. In  
422 support of this, whole genome-duplication, which is common in cancer, has recently  
423 been shown as another potential mechanism that tumor cells could use to maintain  
424 robustness to deleterious passengers<sup>54</sup>. However, duplication events are also known to  
425 be deleterious due to gene dosage effects that cause protein imbalance<sup>55</sup>, which could  
426 further exacerbate protein misfolding. Further experimental studies are needed to  
427 distinguish how cancer cells compensate for protein misfolding and the role that  
428 genome duplication may play in this process.

429 Second, the extra demands of proteostasis maintenance presents important  
430 vulnerabilities in high mutational load cancers that could be exploited. The clinical use of  
431 chaperone inhibitors for cancer treatment has been explored for over two decades<sup>56–58</sup>  
432 but no study, to our knowledge, has compared the efficacy of chaperone inhibitor use in  
433 tumors stratified by mutational load. Similarly, the clinical use of proteasome inhibitors,  
434 which are currently only approved for the treatment of multiple myeloma and mantle-cell  
435 lymphoma<sup>59,60</sup>, has not been directed specifically to high mutational load tumors. While  
436 the efficacy of proteasome inhibitors in multiple myeloma patients is linked to the protein  
437 misfolding stress response<sup>61,62</sup>, it is currently unknown whether high mutational load  
438 tumors are more susceptible to these inhibitors. Outside of drugs in the clinic, the need  
439 for cancers to compensate for protein misfolding could also present additional  
440 vulnerabilities due to evolutionary trade-offs, where the improvement in fitness of one  
441 trait comes at the expense of another. Previous work in yeast has identified strong  
442 trade-offs between the adaptive mechanisms that allow for the tolerance of  
443 mistranslation and survival under conditions of starvation<sup>49</sup>. Whether similar conditions  
444 could be exploited in high mutational load cancer cells warrants additional further  
445 investigation.

446 Finally, our results contribute to an accumulating body of evidence that cancer  
447 and aging are different manifestations of related underlying evolutionary processes<sup>63–65</sup>.  
448 The same forces of mutation and inefficient selection in somatic evolution generates a  
449 persistent problem of deleterious mutation accumulation in normal somatic tissues and  
450 during tumor growth. Disruption of proteostasis is a known hallmark of aging in normal  
451 tissues<sup>66</sup>. Many transcriptional responses observed in high mutational load tumors —  
452 such as shifts in regulation of alternative splicing<sup>67</sup>, protein degradation<sup>68</sup>, and protein  
453 re-folding<sup>69</sup> — are also observed in normal aging tissues which contain somatic  
454 mutations. Despite this, aging tissues appear to utilize different strategies to deal with  
455 proteostasis disruption — such as up-regulation of chaperones in the Small HS family<sup>70</sup>  
456 and autophagy<sup>71</sup> — which are not a pre-dominant response observed here in high  
457 mutational load tumors. Whether different combinations of strategies are used by high



458 mutational load cancer cells use to overcome their mutational load or whether all the  
459 strategies identified here are needed to maintain proteostasis is unclear. Differences in  
460 these proteostasis strategies could be due to different selection pressures during  
461 somatic evolution, the degree of mutational load required to induce a stress response,  
462 differences in energetic costs of protein maintenance, or the interplay that exists  
463 between apoptosis and proteostasis. Further studies are needed to elucidate the  
464 precise dynamics and physiological consequences of inefficient negative selection in  
465 somatic evolution, how this impacts cellular growth, and the mechanisms somatic cells  
466 use to maintain robustness to proteostasis disruption.

## 467 Acknowledgements

468 We thank Kathleen Houlahan, Chuan Li, José Aguilar-Rodríguez and other members of  
469 Petrov and Curtis labs for their helpful comments and discussions. S.T. was supported  
470 in part by an NIH training grant T32-HG000044-21. This work was supported in part by  
471 the National Institutes of Health (NIH) Director's Pioneer Award: DP1CA238296 and the  
472 National Cancer Institute (NCI) Cancer Target Discovery and Development Center  
473 (U01CA217851) to C.C and by NIH grants R35GM118165 to D.A.P and GM74074 to  
474 J.F.

## 475 Conflicts of Interest

476 C.C. is an advisor and stockholder in Grail, Ravel, DeepCell and an advisor to  
477 Genentech, Bristol Myers Squibb, 3T Biosciences and NanoString. D.A.P. is a founder  
478 of, and stockholder equity in, D2G Oncology 42 Inc.

## 479 Methods

480 **Data availability and resources.** Whole-exome, somatic mutation calls of 10,486  
481 cancer patients across 33 cancer types in The Cancer Genome Atlas (TCGA) were  
482 downloaded from the Multi-Center Mutation Calling in Multiple Cancers (MC3) project<sup>16</sup>  
483 (<https://gdc.cancer.gov/about-data/publications/mc3-2017>). For the same patients in  
484 TCGA, RNA-seq data of log<sub>2</sub> transformed RSEM normalized counts were downloaded  
485 from the UCSC Xena Browser<sup>72</sup> (<https://xenabrowser.net/datapages/>) and copy number  
486 alterations (CNAs), including amplifications and deletions, called via ABSOLUTE were  
487 downloaded from COSMIC (v91)<sup>73</sup> (<https://cancer.sanger.ac.uk/cosmic/download>).  
488 Tumor purity estimates for TCGA were downloaded from the Genomic Database  
489 Commons (GDC)<sup>74</sup> (<https://gdc.cancer.gov/about-data/publications/pancanatlas>). Data  
490 for all cancer cell lines in the Cancer Cell Line Encyclopedia (CCLE) were downloaded  
491 from DepMap<sup>30</sup> (<https://depmap.org/portal/download/all/>). Specifically, mutation calls  
492 (Version 21Q3) from whole-exome sequencing data, copy number alternations  
493 quantified by ABSOLUTE (Version CCLE 2019), log<sub>2</sub> transformed TPM normalized  
494 counts (Version 21Q3) from RNA-seq data, shRNA data from project Achilles<sup>32</sup>  
495 normalized using DEMETER (DEMETTER2 Data v6), and primary drug sensitivity

496 screens of replicate collapsed log fold changes relative to DMSO from project PRISM<sup>34</sup>  
497 (Version 19Q4) were used.

498 **Statistical analysis.** The lmerTest and lmer package in R was used to apply a separate  
499 generalized linear mixed model (GLMM) for each gene in the genome to identify groups  
500 of genes whose expression is up-regulated in response to mutational load in TCGA. For  
501 each gene, expression values across all patients were z-score normalized in all  
502 analyses to ensure fair comparisons across genes. Known co-variables of tumor purity  
503 and cancer type were included in the GLMM. Tumor purity and mutational load were  
504 modeled as fixed effects, whereas cancer type was modeled as a random effect (i.e.  
505 random intercept) since it varies across groups of patients and can be interpreted as  
506 repeated measurements across groups. For all analyses, mutational load was defined  
507 as  $\log_{10}$  of the number of synonymous, nonsynonymous and nonsense mutations per  
508 tumor. For each gene, the parameters used in the GLMM were as follows,

$$509 \quad Y \sim \beta_0 + \beta_1 X_1 + \beta_2 X_2 + v + e$$

510 where  $Y$  is a vector of expression values of each tumor,  $\beta_0$  is the fixed intercept,  $\beta_1$  is  
511 the fixed slope for the predictor variable  $X_1$  which is a vector of mutational load values  
512 for each tumor,  $\beta_2$  is the fixed slope for the predictor variable  $X_2$  which is a vector of the  
513 purity of each tumor,  $v$  is the random intercept for each cancer type, and  $e$  is a  
514 Gaussian error term.

515 Unlike TCGA, samples within each cancer type in CCLE can be small and are  
516 unbalanced (i.e. some cancer types have <10 samples and others have >100 samples).  
517 In these cases, mixed effects models may not be able to estimate among-population  
518 variance accurately<sup>31</sup>. Thus, for all regression-based analyses in CCLE, a simple  
519 generalized linear model (GLM) was used instead. Cell viability values across all cell  
520 lines were z-score normalized by gene in all analyses to ensure fair comparisons across  
521 genes. To assess whether the same sets of genes are up-regulated in response to  
522 mutational load in CCLE using the GLM, a similar procedure to the GLMM was  
523 performed. A separate GLM was applied for each gene with the following parameters,

$$524 \quad Y \sim \beta_0 + \beta_1 X_1 + e$$

525 where  $Y$  is a vector normalized expression values of each cell line,  $\beta_0$  is the fixed  
526 intercept,  $\beta_1$  is the fixed slope for the predictor variable  $X_1$  which is a vector of mutational  
527 load values for each tumor, and  $e$  is a Gaussian error term. A similar GLM framework as  
528 above was used to estimate the association of mutational load and cell viability after  
529 shRNA knock-down of individual genes in proteostasis complexes with the following  
530 parameters,

$$531 \quad Y \sim \beta_0 + \beta_1 X_1 + \beta_2 X_2 + e$$

532  
533 where  $Y$  is a vector of normalized cell viability estimates after expression knock-down of  
534 an individual gene across all cell lines,  $\beta_0$  is the fixed reference intercept,  $\beta_1$  is the fixed  
535 slope for the predictor variable  $X_1$  which is a vector of mutational load values for each  
536 cell line,  $\beta_2$  is a change in the intercept for  $X_2$  which is a categorical variable of individual  
537 genes within each proteostasis complex, and  $e$  is a Gaussian error term. To estimate

538 the association of mutational load and cell viability after pharmacologic inhibition of  
539 proteostasis machinery, the following GLM was applied to each relevant drug in PRISM:

540 
$$Y \sim \beta_0 + \beta_1 X_1 + e$$

541 where  $Y$  is a vector normalized cell viability estimates after drug inhibition across all cell  
542 lines,  $\beta_0$  is the fixed intercept,  $\beta_1$  is the fixed slope for the predictor variable  $X_1$  which is a  
543 vector of mutational load values for each tumor, and  $e$  is a Gaussian error term.

544  
545 **Model validation.** For both the GLM and GLMM, model assumptions of homogeneity of  
546 variance were verified by plotting residuals versus fitted values in the model and  
547 residuals versus each covariate in the model. Multi-collinearity with other mutational  
548 classes (e.g. such as copy number alterations, CNAs) were considered but not found to  
549 correlate with point mutations (Supplemental Figure 1). A jackknife re-sampling  
550 procedure was used for outlier analysis and to determine whether specific cancer types  
551 are driving patterns of association within the GLM and GLMM. Briefly, each cancer type  
552 was removed from the regression model one at a time, and regression coefficients were  
553 re-estimated. Overall, regression coefficients were fairly stable across cancer types and  
554 trends remained the same (Supplemental Figure 4 and 6).

555 **Proteostasis gene sets.** Genes for chaperone complexes were identified from<sup>75</sup> and  
556 genes that are co-chaperones were not considered. Proteasome and ribosomal  
557 complexes were identified from CORUM<sup>17</sup>.

558 **Gene set enrichment analysis.** All gene set enrichment analysis was performed using  
559 gprofiler2 with default parameters. For all sets of genes, significance was determined  
560 after correcting for multiple hypothesis testing (FDR < 0.05). For gene set enrichment  
561 analysis used to identify genes up-regulated in TCGA in response to mutational load, all  
562 terms in CORUM database were reported and enrichment terms in the KEGG database  
563 of diseases not related to cancer (e.g. 'Influenza A') were omitted from the main figures  
564 for clarity and space. For gene sets used to identify terms differentially splice in between  
565 high and low mutational load tumors, all terms in the CORUM and the REACTOME  
566 database were reported in the main figures. The full set of enrichment terms for all  
567 analyses is reported in Supplemental Table 1.

568 **Alternative splicing analysis.** Alternative splicing events were quantified through a  
569 previously established metric called PSI. PSI is calculated as the number of reads that  
570 overlap the alternative splicing event (e.g. for intron retention, either at intronic regions  
571 or those at the boundary of exon to intron junctions) divided by the total number of  
572 reads that support and don't support the alternative splicing event. PSI summarizes  
573 alternative splicing events at specific exonic boundaries in the entire transcript  
574 population without needing to know the complete underlying composition of each full  
575 length-transcript.

576 Alternative splicing calls for all tumors in TCGA were downloaded from TCGA  
577 SpliceSeq<sup>25</sup>. Default splice event filters (percentage of samples with PSI values >75%)

578 from the database were applied. To test whether gene expression is down-regulated in  
579 high mutational load tumors through alternative splicing, we calculated whether  
580 alternative splicing events were present based on different threshold values of percent  
581 spliced in (PSI) from 90% to 50%. (Supplemental Figure 3). For each alternative splicing  
582 event in a gene, we quantified whether the expression of the same gene was under-  
583 expressed. Each gene was counted as under-expressed if it was one standard deviation  
584 below the mean expression within each cancer type. Genes that contained a point  
585 mutation within the same alternative splicing event were removed to control for eQTL  
586 effects. We note that intron retention events removed from this analysis represent only  
587 ~1% of intron retention events across all tumors and similar trends are found when this  
588 filtering scheme is not applied (Supplemental Figure 2). In addition, we evaluated  
589 whether this trend is robust to other alternative splicing events (i.e., Alternate Donor  
590 Sites, Alternate Promoters, Alternate Terminators, Exon Skipping Events, ME=Mutually  
591 Exclusive Exon; Supplemental Figure 3).

592 To investigate which genes are differentially spliced in between low and high  
593 mutational load tumors for specific alternative splicing events (i.e. intron retention), a t-  
594 test was used to calculate whether PSI values were significantly different in tumors with  
595 < 10 protein-coding mutations compared to tumors with > 1000 protein-coding  
596 mutations. Each alternative splicing event within a gene was required to have less than  
597 25% of missing PSI values and a mean difference between the two groups of >0.01 to  
598 be considered. This approach identified 606 and 201 significant genes that have more  
599 and fewer intron retention events in high mutational load tumors, respectively, after  
600 correcting for multiple hypothesis testing (FDR < 0.05).

601  
602 **Drug category annotation and enrichment analysis.** A separate GLM was ran for all  
603 drugs in the PRISM database to evaluate whether they are associated with mutational  
604 load and cell viability. All drugs that were negatively associated with mutational load and  
605 viability were queried on PubMed based on their reported mechanism of action in  
606 PRISM and grouped into broad categories (Supplemental Table 1). Categories of drug  
607 mechanism of action were first chosen based on their role in metabolism and known  
608 hallmarks of cancer. Additional categories not directly related to known cancer  
609 associated functional groups were made for drugs that could not otherwise be grouped  
610 (i.e. 'Ion Channel Regulation', 'Viral Replication Inhibitor', etc.). Drugs with ambiguous  
611 mechanism of action (e.g. 'cosmetic', 'coloring agent') were grouped into 'Other'. The  
612 abstracts of up to 10 associated papers were used to examine for evidence connecting  
613 drug mechanisms of action to 33 broad categories. In total, 700 drug mechanism of  
614 action were grouped and annotated into 33 broad categories. These broad categories  
615 were used to assess whether high mutational load cancer cell lines are generically  
616 vulnerable to drugs or whether certain categories are more likely to contain drugs  
617 effective against high mutational load cell lines. To control for differences in the number  
618 of drugs within each category, 50 drugs were randomly sampled, and the fraction of  
619 drugs significantly associated with mutational load in each category was calculated 100  
620 times to generate confidence intervals.

621 **Code and software availability.** All code used for analysis will be made publicly  
622 available on Github under the open-source MIT License upon publication.

623

624

625

626

627

628

629

630

631

632

633

634

635

636

637

638

639

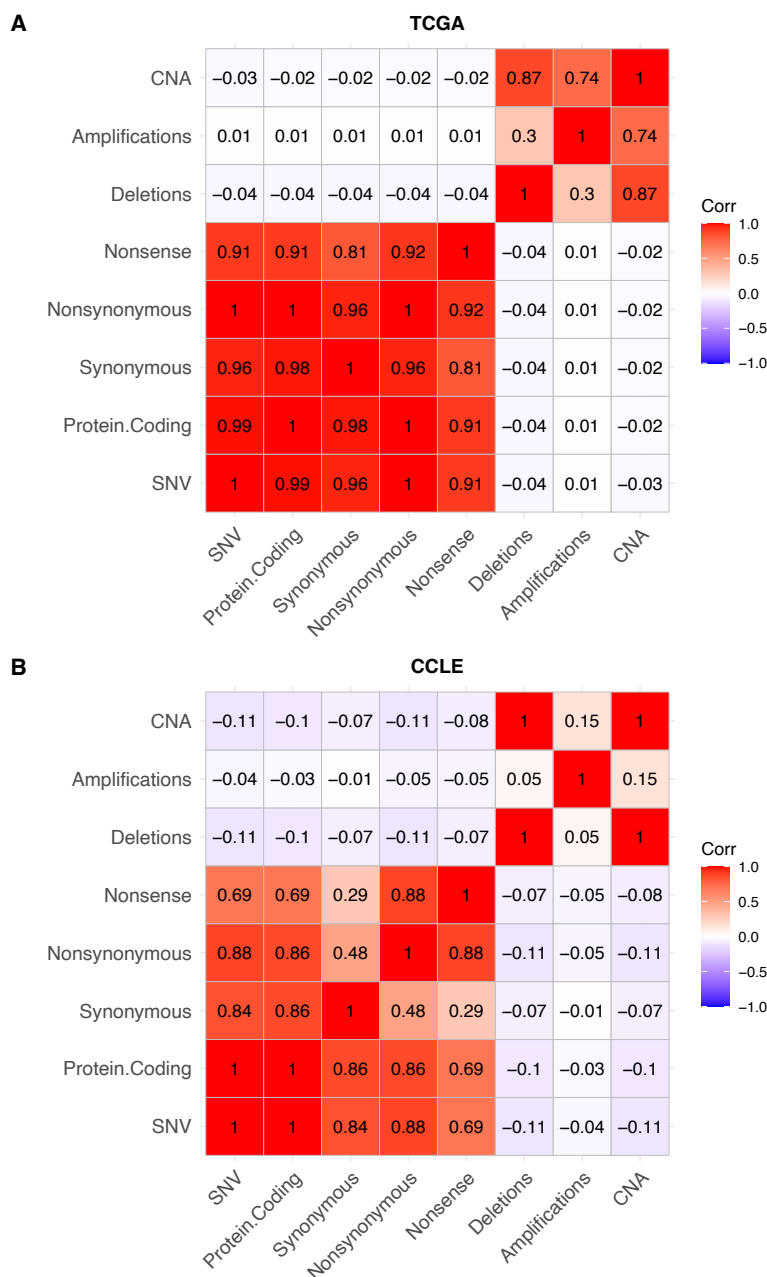
640

641

642



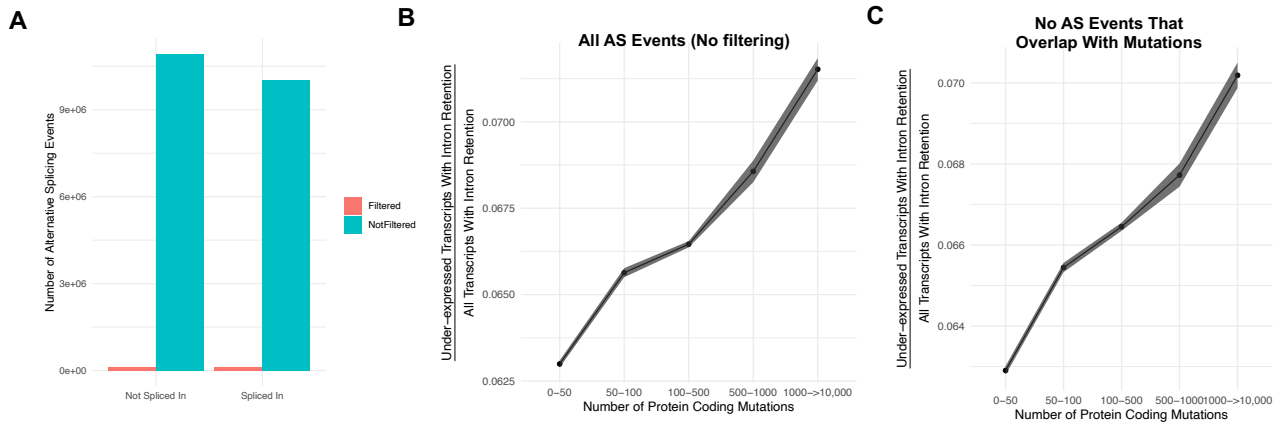
643  
644 **Supplemental Figures**  
645



646  
647 **Supplemental Figure 1. No collinearity of point mutations and copy number alterations in human**  
648 **tumors (TCGA) and cancer cell lines (CCLE).** Heatmap of Pearson's correlation coefficients between  
649 different classes of mutations in **A. CCLE** (cancer cell lines) and **B. TCGA** (human tumors). Colors denote  
650 magnitude of correlation coefficients and whether the relationship is positive (red), negative (blue) or  
651 negligible (white). CNAs are defined as the combined number of amplifications and deletions, while SNVs  
652 are the combined number of all point mutations.

653

654



655 **Supplemental Figure 2. Intron retention events that overlap with mutations do not account for the**  
656 **association of gene silencing in high mutational load tumors. A.** Counts of the number of intron  
657 retention events filtered (in red) due to overlap with a mutation present in the same gene (and thus  
658 corresponding to potential eQTLs) compared the number of remaining alternative splicing events with no  
659 overlap with a mutation (in blue). Alternative splicing events filtered represent ~1% of all alternative  
660 splicing events across all tumors. **B-C.** Counts of the number of under-expressed transcripts with intron  
661 retention events, relative to counts of all intron retention events in tumors binned by the total number of  
662 protein-coding mutations. Shown are when trends when **(B)** not filtering alternative splicing events due to  
663 overlap with mutations and **(C)** when events are filtered (same as Fig. 2A). Intron retention events with  
664 PSI > 80% are counted. Error bars are 95% confidence intervals determined by bootstrap sampling.  
665 These results further support the prediction that gene silencing is elevated in high mutational load tumors  
666 and likely mediated by the coupling of intron retention with mRNA decay

667

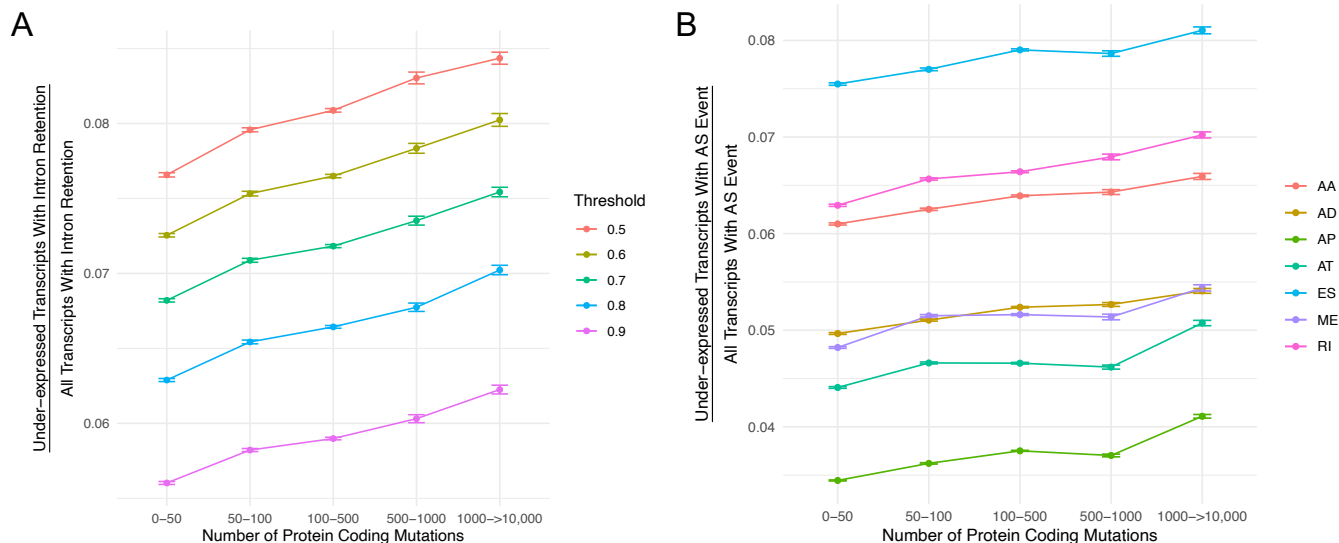
668

669

670

671

672

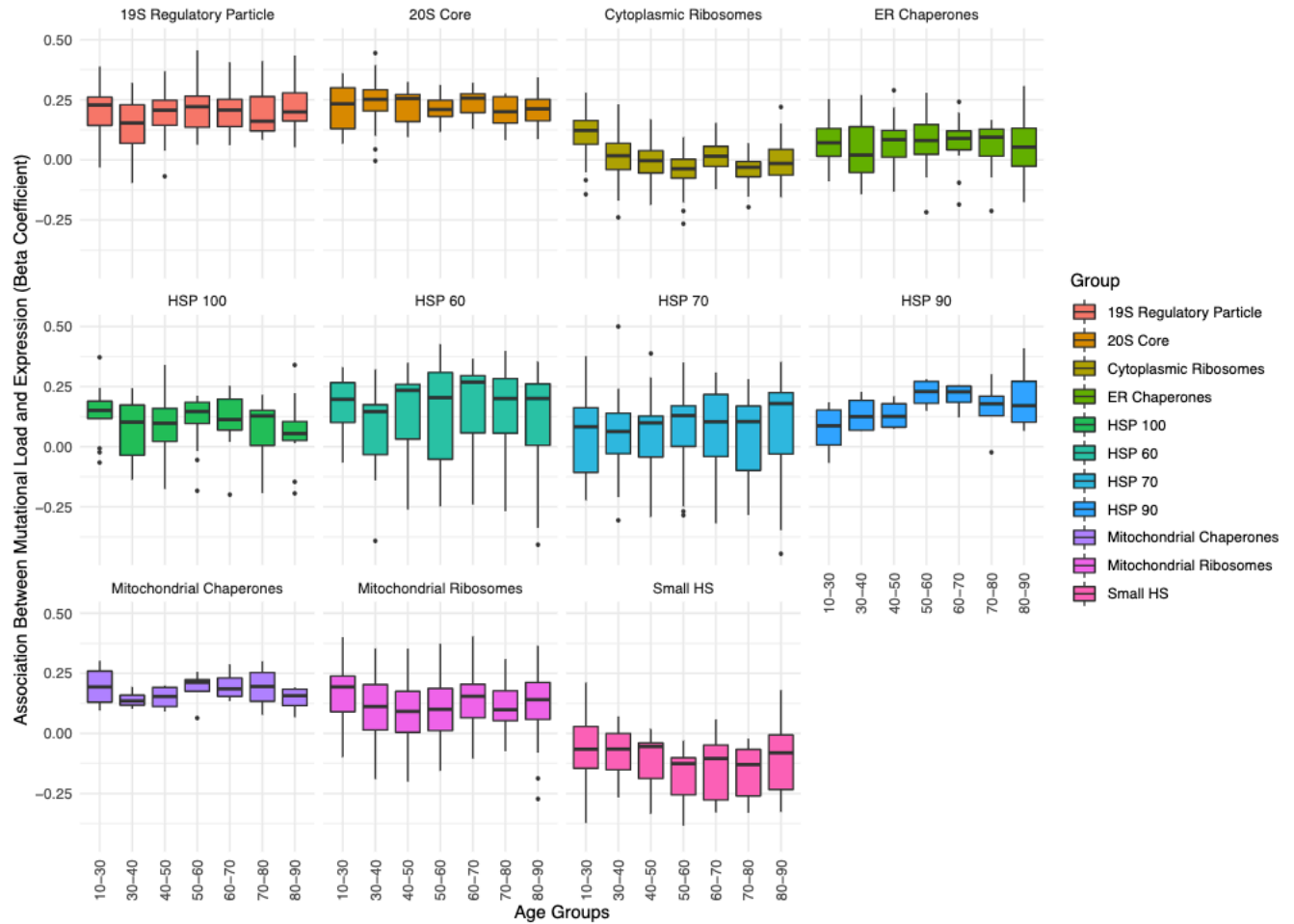


673

674 **Supplemental Figure 3. The number of under-expressed transcripts increases with the mutational**  
 675 **load of tumors for different PSI value thresholds and alternative splicing events. A.** Counts of the  
 676 number of under-expressed transcripts with intron retention events, relative to counts of all intron  
 677 retention events in tumors binned by the total number of protein-coding mutations. Intron retention events  
 678 with different PSI thresholds are shown colored. **B.** Counts of the number of under-expressed transcripts  
 679 that contain different classes alternative splicing events, relative to counts of all alternative splicing events  
 680 of the same class in tumors binned by the total number of protein-coding mutations. Alternative splicing  
 681 events of different classes are shown colored (AA=Alternate Acceptor Sites, AD=Alternate Donor Sites,  
 682 AP=Alternate Promoter, AT=Alternate Terminator, ES=Exon Skip, ME=Mutually Exclusive Exons, RI=  
 683 Retained Intron). Error bars are 95% confidence intervals determined by bootstrap sampling.

684



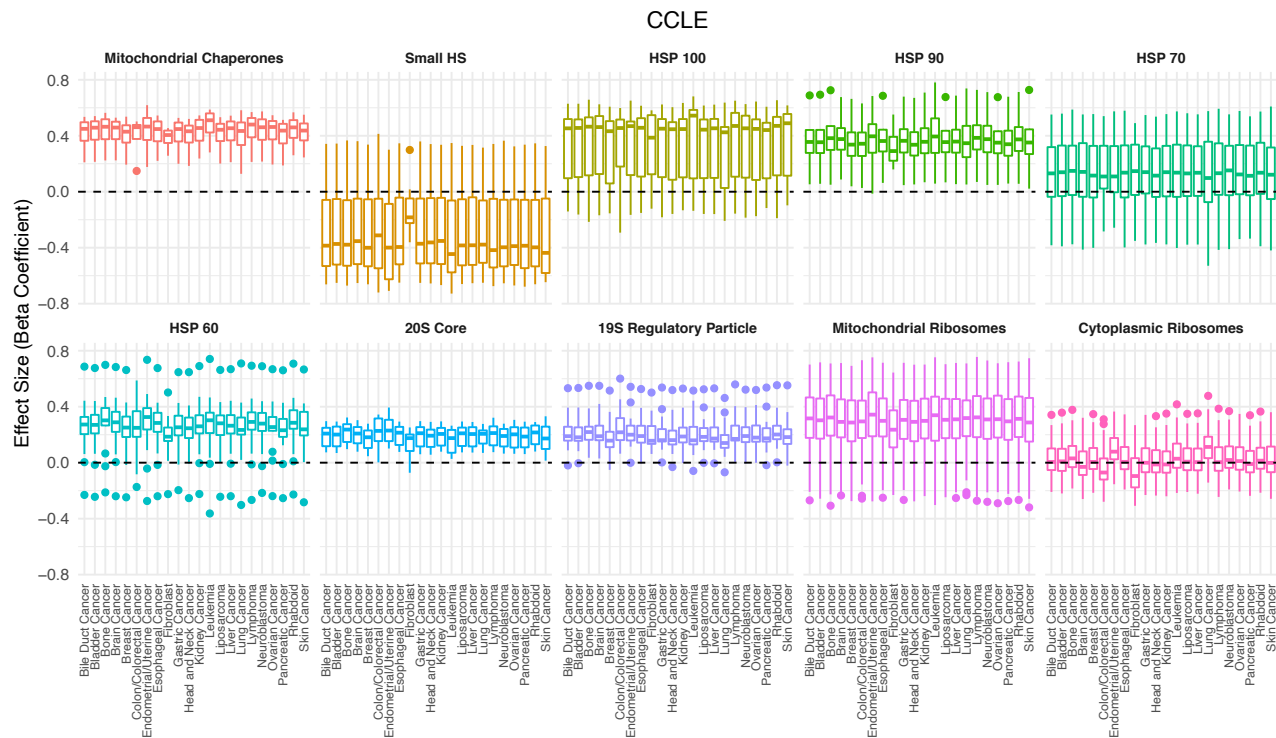


692

693 **Supplemental Figure 5. Association between the expression in proteostasis complexes and**  
694 **mutational load is not driven by patient age.** Boxplots of regression coefficients from the GLMM  
695 measuring the association of the expression of each individual gene with the mutational load of tumors  
696 from TCGA colored by different proteostasis complexes. Shown are regression coefficients when running  
697 the GLMM on tumors stratified by different age groups (x-axis).

698





699

700 **Supplemental Figure 6. Association between the expression in proteostasis complexes and**  
 701 **mutational load is not driven by a single cancer type in CCLE.** Box plots of regression coefficients  
 702 from the GLM measuring the association of the expression of each individual gene with the mutational  
 703 load of tumors colored by different proteostasis complexes. Shown are regression estimates after  
 704 removing each cancer type in CCLE (x-axis) and re-running the GLM.

705

706

707

708

709

710

711

712

713

714

715

## 716 References

- 717 1. Lawrence, M. S. *et al.* Mutational heterogeneity in cancer and the search for new cancer-  
718 associated genes. *Nature* (2013) doi:10.1038/nature12213.
- 719 2. Bakhoun, S. F. & Landau, D. A. Cancer Evolution: No Room for Negative Selection. *Cell* (2017)  
720 doi:10.1016/j.cell.2017.10.039.
- 721 3. Martincorena, I. *et al.* Universal Patterns of Selection in Cancer and Somatic Tissues. *Cell* (2017)  
722 doi:10.1016/j.cell.2017.09.042.
- 723 4. Bozic, I., Paterson, C. & Waclaw, B. On measuring selection in cancer from subclonal mutation  
724 frequencies. *PLoS Comput. Biol.* (2019) doi:10.1371/journal.pcbi.1007368.
- 725 5. McFarland, C. D. *et al.* The damaging effect of passenger mutations on cancer progression.  
726 *Cancer Res.* (2017) doi:10.1158/0008-5472.CAN-15-3283-T.
- 727 6. McFarland, C. D., Korolev, K. S., Kryukov, G. V., Sunyaev, S. R. & Mirny, L. A. Impact of  
728 deleterious passenger mutations on cancer progression. *Proc. Natl. Acad. Sci. U. S. A.* (2013)  
729 doi:10.1073/pnas.1213968110.
- 730 7. Zapata, L. *et al.* Negative selection in tumor genome evolution acts on essential cellular functions  
731 and the immunopeptidome. *Genome Biol.* (2018) doi:10.1186/s13059-018-1434-0.
- 732 8. Williams, M. J., Werner, B., Barnes, C. P., Graham, T. A. & Sottoriva, A. Identification of neutral  
733 tumor evolution across cancer types. *Nat. Genet.* (2016) doi:10.1038/ng.3489.
- 734 9. Neutral Theory and the Somatic Evolution of Cancer. *Mol. Biol. Evol.* (2018)  
735 doi:10.1093/molbev/msy100.
- 736 10. Tilk, S., Curtis, C., Petrov, D. A. & McFarland, C. D. Most cancers carry a substantial deleterious  
737 load due to Hill-Robertson interference. *bioRxiv* (2019) doi:10.1101/764340.
- 738 11. Eyre-Walker, A. & Keightley, P. D. The distribution of fitness effects of new mutations. *Nature*  
739 *Reviews Genetics* (2007) doi:10.1038/nrg2146.
- 740 12. Martincorena, I. *et al.* Universal Patterns of Selection in Cancer and Somatic Tissues. *Cell* (2017)  
741 doi:10.1016/j.cell.2017.09.042.
- 742 13. Drummond, D. A. & Wilke, C. O. Mistranslation-induced protein misfolding as a dominant  
743 constraint on coding-sequence evolution. *Cell* **134**, 341–52 (2008).
- 744 14. Hill, W. G. & Robertson, A. The effect of linkage on limits to artificial selection. *Genet. Res.*  
745 (*Camb.*) (2008) doi:10.1017/S001667230800949X.
- 746 15. Weinstein, J. N. *et al.* The cancer genome atlas pan-cancer analysis project. *Nat. Genet.* (2013)  
747 doi:10.1038/ng.2764.
- 748 16. Ellrott, K. *et al.* Scalable Open Science Approach for Mutation Calling of Tumor Exomes Using  
749 Multiple Genomic Pipelines. *Cell Syst.* **6**, 271–281.e7 (2018).
- 750 17. Giurgiu, M. *et al.* CORUM: The comprehensive resource of mammalian protein complexes - 2019.  
751 *Nucleic Acids Res.* (2019) doi:10.1093/nar/gky973.
- 752 18. Tanabe, M. & Kanehisa, M. Using the KEGG database resource. *Curr. Protoc. Bioinforma.* (2012)  
753 doi:10.1002/0471250953.bi0112s38.
- 754 19. Peterson, H., Kolberg, L., Raudvere, U., Kuzmin, I. & Vilo, J. gprofiler2 -- an R package for gene  
755 list functional enrichment analysis and namespace conversion toolset g: Profiler. *F1000Research*  
756 (2020) doi:10.12688/f1000research.24956.2.
- 757 20. Biamonti, G. & Caceres, J. F. Cellular stress and RNA splicing. *Trends in Biochemical Sciences*  
758 (2009) doi:10.1016/j.tibs.2008.11.004.
- 759 21. Dutertre, M., Sanchez, G., Barbier, J., Corcos, L. & Auboeuf, D. The emerging role of pre-  
760 messenger RNA splicing in stress responses: Sending alternative messages and silent  
761 messengers. *RNA Biology* (2011) doi:10.4161/rna.8.5.16016.
- 762 22. Ge, Y. & Porse, B. T. The functional consequences of intron retention: Alternative splicing coupled  
763 to NMD as a regulator of gene expression. *BioEssays* (2014) doi:10.1002/bies.201300156.
- 764 23. Lindeboom, R. G. H., Supek, F. & Lehner, B. The rules and impact of nonsense-mediated mRNA  
765 decay in human cancers. *Nat. Genet.* (2016) doi:10.1038/ng.3664.
- 766 24. Lareau, L. F., Inada, M., Green, R. E., Wengrod, J. C. & Brenner, S. E. Unproductive splicing of  
767 SR genes associated with highly conserved and ultraconserved DNA elements. *Nature* (2007)  
768 doi:10.1038/nature05676.
- 769 25. Ryan, M. *et al.* TCGASpliceSeq a compendium of alternative mRNA splicing in cancer. *Nucleic*  
770 *Acids Res.* (2016) doi:10.1093/nar/gkv1288.

- 771 26. Sun, Y. & MacRae, T. H. The small heat shock proteins and their role in human disease. *FEBS*  
772 *Journal* (2005) doi:10.1111/j.1742-4658.2005.04708.x.
- 773 27. Ruan, L. *et al.* Cytosolic proteostasis through importing of misfolded proteins into mitochondria.  
774 *Nature* (2017) doi:10.1038/nature21695.
- 775 28. Shcherbakov, D. *et al.* Ribosomal mistranslation leads to silencing of the unfolded protein  
776 response and increased mitochondrial biogenesis. *Commun. Biol.* (2019) doi:10.1038/s42003-  
777 019-0626-9.
- 778 29. Stein, K. C. & Frydman, J. The stop-and-go traffic regulating protein biogenesis: How translation  
779 kinetics controls proteostasis. *Journal of Biological Chemistry* (2019)  
780 doi:10.1074/jbc.REV118.002814.
- 781 30. Barretina, J. *et al.* The Cancer Cell Line Encyclopedia enables predictive modelling of anticancer  
782 drug sensitivity. *Nature* (2012) doi:10.1038/nature11003.
- 783 31. Harrison, X. A. *et al.* A brief introduction to mixed effects modelling and multi-model inference in  
784 ecology. *PeerJ* (2018) doi:10.7717/peerj.4794.
- 785 32. Tsherniak, A. *et al.* Defining a Cancer Dependency Map. *Cell* (2017)  
786 doi:10.1016/j.cell.2017.06.010.
- 787 33. Zolkiewski, M., Zhang, T. & Nagy, M. Aggregate reactivation mediated by the Hsp100 chaperones.  
788 *Archives of Biochemistry and Biophysics* (2012) doi:10.1016/j.abb.2012.01.012.
- 789 34. Corsello, S. M. *et al.* Discovering the anticancer potential of non-oncology drugs by systematic  
790 viability profiling. *Nat. Cancer* (2020) doi:10.1038/s43018-019-0018-6.
- 791 35. Kristofich, J. C. *et al.* Synonymous mutations make dramatic contributions to fitness when growth  
792 is limited by a weak-link enzyme. *PLoS Genet.* (2018) doi:10.1371/journal.pgen.1007615.
- 793 36. Spencer, P. S., Siller, E., Anderson, J. F. & Barral, J. M. Silent substitutions predictably alter  
794 translation elongation rates and protein folding efficiencies. *J. Mol. Biol.* (2012)  
795 doi:10.1016/j.jmb.2012.06.010.
- 796 37. Zhang, G., Hubalewska, M. & Ignatova, Z. Transient ribosomal attenuation coordinates protein  
797 synthesis and co-translational folding. *Nat. Struct. Mol. Biol.* (2009) doi:10.1038/nsmb.1554.
- 798 38. Walsh, I. M., Bowman, M. A., Soto Santarriaga, I. F., Rodriguez, A. & Clark, P. L. Synonymous  
799 codon substitutions perturb cotranslational protein folding in vivo and impair cell fitness. *Proc. Natl.*  
800 *Acad. Sci. U. S. A.* (2020) doi:10.1073/pnas.1907126117.
- 801 39. Plotkin, J. B. & Kudla, G. Synonymous but not the same: The causes and consequences of codon  
802 bias. *Nature Reviews Genetics* (2011) doi:10.1038/nrg2899.
- 803 40. Bobula, J. *et al.* Why molecular chaperones buffer mutational damage: A case study with a yeast  
804 Hsp40/70 system. *Genetics* (2006) doi:10.1534/genetics.106.061564.
- 805 41. Maisnier-Patin, S. *et al.* Genomic buffering mitigates the effects of deleterious mutations in  
806 bacteria. *Nat. Genet.* (2005) doi:10.1038/ng1676.
- 807 42. Fares, M. A., Ruiz-González, M. X., Moya, A., Elena, S. F. & Barrio, E. Endosymbiotic bacteria:  
808 GroEL buffers against deleterious mutations. *Nature* (2002) doi:10.1038/417398a.
- 809 43. Elena, S. F., Carrasco, P., Daròs, J. A. & Sanjuán, R. Mechanisms of genetic robustness in RNA  
810 viruses. *EMBO Reports* (2006) doi:10.1038/sj.embor.7400636.
- 811 44. Pan, Q. *et al.* Quantitative microarray profiling provides evidence against widespread coupling of  
812 alternative splicing with nonsense-mediated mRNA decay to control gene expression. *Genes Dev.*  
813 (2006) doi:10.1101/gad.1382806.
- 814 45. Green, R. E. *et al.* Widespread predicted nonsense-mediated mRNA decay of alternatively-spliced  
815 transcripts of human normal and disease genes. in *Bioinformatics* (2003).  
816 doi:10.1093/bioinformatics/btg1015.
- 817 46. Cuccurese, M., Russo, G., Russo, A. & Pietropaolo, C. Alternative splicing and nonsense-  
818 mediated mRNA decay regulate mammalian ribosomal gene expression. *Nucleic Acids Res.*  
819 (2005) doi:10.1093/nar/gki905.
- 820 47. Mitrovich, Q. M. & Anderson, P. Unproductively spliced ribosomal protein mRNAs are natural  
821 targets of mRNA surveillance in *C. elegans*. *Genes Dev.* (2000) doi:10.1101/gad.819900.
- 822 48. Parenteau, J. *et al.* Introns within ribosomal protein genes regulate the production and function of  
823 yeast ribosomes. *Cell* (2011) doi:10.1016/j.cell.2011.08.044.
- 824 49. Kalapis, D. *et al.* Evolution of Robustness to Protein Mistranslation by Accelerated Protein  
825 Turnover. *PLoS Biol.* (2015) doi:10.1371/journal.pbio.1002291.
- 826 50. Tokheim, C. *et al.* Systematic characterization of mutations altering protein degradation in human

- 827 cancers. *Mol. Cell* (2021) doi:10.1016/j.molcel.2021.01.020.
- 828 51. Martínez-Jiménez, F., Muiños, F., López-Arribillaga, E., Lopez-Bigas, N. & Gonzalez-Perez, A.  
829 Systematic analysis of alterations in the ubiquitin proteolysis system reveals its contribution to  
830 driver mutations in cancer. *Nat. Cancer* (2020) doi:10.1038/s43018-019-0001-2.
- 831 52. Conant, G. C. & Wagner, A. Duplicate genes and robustness to transient gene knock-downs in  
832 *Caenorhabditis elegans*. *Proc. R. Soc. B Biol. Sci.* (2004) doi:10.1098/rspb.2003.2560.
- 833 53. Gu, Z. *et al.* Role of duplicate genes in genetic robustness against null mutations. *Nature* (2003).
- 834 54. López, S. *et al.* Interplay between whole-genome doubling and the accumulation of deleterious  
835 alterations in cancer evolution. *Nat. Genet.* (2020) doi:10.1038/s41588-020-0584-7.
- 836 55. Torres, E. M. *et al.* Effects of aneuploidy on cellular physiology and cell division in haploid yeast.  
837 *Science* (80-. ). (2007) doi:10.1126/science.1142210.
- 838 56. Neckers, L. & Workman, P. Hsp90 molecular chaperone inhibitors: Are we there yet? *Clinical*  
839 *Cancer Research* (2012) doi:10.1158/1078-0432.CCR-11-1000.
- 840 57. Pacey, S., Banerji, U., Judson, I. & Workman, P. Hsp90 inhibitors in the clinic. *Handbook of*  
841 *experimental pharmacology* (2006).
- 842 58. Kim, Y. *et al.* Update on Hsp90 Inhibitors in Clinical Trial. *Curr. Top. Med. Chem.* (2009)  
843 doi:10.2174/156802609789895728.
- 844 59. Manasanch, E. E. & Orlowski, R. Z. Proteasome inhibitors in cancer therapy. *Nature Reviews*  
845 *Clinical Oncology* (2017) doi:10.1038/nrclinonc.2016.206.
- 846 60. Park, J. E., Miller, Z., Jun, Y., Lee, W. & Kim, K. B. Next-generation proteasome inhibitors for  
847 cancer therapy. *Translational Research* (2018) doi:10.1016/j.trsl.2018.03.002.
- 848 61. Bianchi, G. *et al.* The proteasome load versus capacity balance determines apoptotic sensitivity of  
849 multiple myeloma cells to proteasome inhibition. *Blood* (2009) doi:10.1182/blood-2008-08-172734.
- 850 62. Ling, S. C. W. *et al.* Response of myeloma to the proteasome inhibitor bortezomib is correlated  
851 with the unfolded protein response regulator XBP-1. *Haematologica* (2012)  
852 doi:10.3324/haematol.2011.043331.
- 853 63. Martincorena, I. *et al.* Somatic mutant clones colonize the human esophagus with age. *Science*  
854 (80-. ). (2018) doi:10.1126/science.aau3879.
- 855 64. Martincorena, I. *et al.* High burden and pervasive positive selection of somatic mutations in normal  
856 human skin. *Science* (80-. ). (2015) doi:10.1126/science.aaa6806.
- 857 65. Kennedy, S. R., Zhang, Y. & Risques, R. A. Cancer-Associated Mutations but No Cancer: Insights  
858 into the Early Steps of Carcinogenesis and Implications for Early Cancer Detection. *Trends in*  
859 *Cancer* (2019) doi:10.1016/j.trecan.2019.07.007.
- 860 66. López-Otín, C., Blasco, M. A., Partridge, L., Serrano, M. & Kroemer, G. The hallmarks of aging.  
861 *Cell* (2013) doi:10.1016/j.cell.2013.05.039.
- 862 67. Adusumalli, S., Ngian, Z. K., Lin, W. Q., Benoukraf, T. & Ong, C. T. Increased intron retention is a  
863 post-transcriptional signature associated with progressive aging and Alzheimer's disease. *Aging*  
864 *Cell* (2019) doi:10.1111/accel.12928.
- 865 68. Löw, P. The role of ubiquitin-proteasome system in ageing. *General and Comparative*  
866 *Endocrinology* (2011) doi:10.1016/j.ygcen.2011.02.005.
- 867 69. Soti, C. & Csermely, P. Aging and molecular chaperones. *Exp. Gerontol.* (2003)  
868 doi:10.1016/S0531-5565(03)00185-2.
- 869 70. Charmpilas, N., Kyriakakis, E. & Tavernarakis, N. Small heat shock proteins in ageing and age-  
870 related diseases. *Cell Stress and Chaperones* (2017) doi:10.1007/s12192-016-0761-x.
- 871 71. Aman, Y. *et al.* Autophagy in healthy aging and disease. *Nat. Aging* (2021) doi:10.1038/s43587-  
872 021-00098-4.
- 873 72. Goldman, M. J. *et al.* Visualizing and interpreting cancer genomics data via the Xena platform.  
874 *Nature Biotechnology* (2020) doi:10.1038/s41587-020-0546-8.
- 875 73. Bamford, S. *et al.* The COSMIC (Catalogue of Somatic Mutations in Cancer) database and  
876 website. *Br. J. Cancer* (2004) doi:10.1038/sj.bjc.6601894.
- 877 74. Grossman, R. L. *et al.* Toward a Shared Vision for Cancer Genomic Data. *N. Engl. J. Med.* **375**,  
878 1109–1112 (2016).
- 879 75. Hadizadeh Esfahani, A., Sverchkova, A., Saez-Rodriguez, J., Schuppert, A. A. & Brehme, M. A  
880 systematic atlas of chaperome deregulation topologies across the human cancer landscape. *PLoS*  
881 *Comput. Biol.* (2018) doi:10.1371/journal.pcbi.1005890.
- 882